octapole. The experimental value for the octapole moment of HMT, derived including all multipole terms up to octapole, is $< xyz > = + 1.4\,(2)|e|\text{Å}^3$, using population parameters obtained without constraint on the o_4 parameters. The corresponding value from Terpstra, Craven & Stewart (1993) is $< xyz > = + 1.0\,(3)|e|\text{Å}^3$. When the o_4 parameters are constrained, the value derived from Table 2, column (*b*), is $1.9\,(2)|e|\text{Å}^3$. Corresponding octapole moments as defined by Buckingham (1970) are $\Omega = \frac{5}{2} < xyz > = - 5.5\,(7)$, $-4.0\,(14)$ and $-7.6\,(6) \times 10^{-49}\ \text{C m}^3$, respectively. Although an increasing number of molecular dipole and quadrupole moments is being reported (Spackman, 1992), HMT appears to provide the first example of a molecular octapole moment determined from Bragg diffraction data.

This work was supported by grants GM-31593 and HL-20350 from the US National Institutes of Health. We are grateful to Mrs Joan Klinger for technical assistance.

References

BLESSING, R. H. (1989). *J. Appl. Cryst.* **22**, 396–397.

BUCKINGHAM, A. D. (1970). In *Physical Chemistry: An Advanced Treatise*, Vol IV, edited by H. EYRING, D. HENDERSON & W. JOST. New York: Academic Press.

BUSING, W. R. & LEVY, H. A. (1957). *Acta Cryst.* **10**, 180–182.

CLEMENTI, C. & ROETTI, C. (1974). *Atomic Data and Nuclear Data Tables*, Vol. 14, pp. 177–178. New York: Academic Press.

COPPENS, P., GURU ROW, T. N., LEUNG, P., STEVENS, E. D., BECKER, P. J. & YANG, Y. W. (1979). *Acta Cryst.* A**35**, 63–72.

CRAVEN, B. M. & WEBER, H. P. (1983). *Acta Cryst.* B**39**, 743–748.

CRAVEN, B. M., WEBER, H. P., HE, X. M. & KLOOSTER, W. (1993). *The POP Procedure, Computer Programs to Derive Electrostatic Properties from Bragg Reflections.* Technical Report, Department of Crystallography, Univ. of Pittsburgh, PA, USA.

CROMER, D. T. & WABER, J. T. (1974). *International Tables for X-ray Crystallography*, Vol. IV, pp. 71–147. Birmingham: Kynoch Press. (Present distributor Kluwer Academic Publishers, Dordrecht.)

DICKINSON, R. G. & RAYMOND, A. L. (1923). *J. Am. Chem. Soc.* **45**, 22–29.

EPSTEIN, J., RUBLE, J. R. & CRAVEN, B. M. (1982). *Acta Cryst.* B**38**, 140–149.

HEHRE, W. J., STEWART, R. F. & POPLE, J. A. (1969). *J. Chem. Phys.* **51**, 2657–2664.

JOHNSON, C. K. (1976). *ORTEP*II. Report ORNL-5138. Oak Ridge National Laboratory, Tennessee, USA.

KAMPERMANN, S. P., SABINE, T. M., CRAVEN, B. M. & MCMULLAN, R. K. (1994). In preparation.

LEHMANN, M. S. & LARSEN, F. K. (1974). *Acta Cryst.* A**30**, 580–584.

SPACKMAN, M. A. (1992). *Chem. Rev.* **92**, 1769–1797.

STEVENS, E. D. & HOPE, H. (1975). *Acta Cryst.* A**31**, 494–498.

STEWART, R. F. (1976). *Acta Cryst.* A**32**, 565–574.

STEWART, R. F. & CRAVEN, B. M. (1993). *Biophys. J.* **65**, 998–1005.

SWAMINATHAN, S. & CRAVEN, B. M. (1984). *Acta Cryst.* B**40**, 511–518.

TERPSTRA, M., CRAVEN, B. M. & STEWART, R. F. (1993). *Acta Cryst.* A**49**, 685–692.

Acta Cryst. (1994). B**50**, 741–746

Electrocrystallization, Crystal Structure and Physical Properties of Hexaperylene Hexafluorophosphate, $(C_{20}H_{12})_6^{\cdot+}PF_6^-$

BY WERNER F. KUHS AND GÜNTER MATTERN

Institut für Kristallographie, Universität Karlsruhe, D-76128 Karlsruhe, Germany

WOLFGANG BRÜTTING

Experimentalphysik II, Universität Bayreuth, D-95440 Bayreuth, Germany

AND HEDWIG DRAGAN, MICHAEL BURGGRAF, BERND PILAWA AND ELMAR DORMANN

Physikalisches Institut, Universität Karlsruhe (TH), D-76128 Karlsruhe, Germany

(*Received* 10 *January* 1994; *accepted* 13 *April* 1994)

Abstract

Electrocrystallization and crystal structure are reported for the 6:1 salt of perylene (PE) and hexafluorophosphate. The three-dimensional crystal structure contains PE dimers with very small intradimer and large interdimer separation. Measurements of static magnetic susceptibility and d.c. electrical conductivity characterize $(PE)_6PF_6$ as an organic semiconductor with comparatively large activation energy and one Curie-like radical spin per formula unit.

1. Introduction

Recently the radical cation salts of aromatic hydrocarbons such as fluoranthene, pyrene or perylene (PE) with inorganic complex anions such as hexafluorophosphate or -arsenate have received considerable interest. A large number of different crystal structures with different stoichiometries can be obtained by electrocrystallization from various solvents. Typically dimers of the flat arenes are stacked with their molecular planes perpendicular to or inclined to the stacking direction, occasionally with additional single arenes surrounding the one-dimensional channels (Endres, Keller, Müller & Schweitzer, 1985; Enkelmann & Göckelmann, 1987). Quasi-one-dimensional room-temperature electrical conductivity is observed in many radical cation salts, with maximum values of 10^2–10^3 S cm^{-1} in the stacking direction and with the anisotropy reaching values of $\sigma_\parallel/\sigma_\perp \approx 10^4$. A Peierls transition to a low-temperature semiconducting or insulating phase is typically observed in the 100–200 K range (Keller *et al.*, 1980; Riess, Brütting & Schwoerer, 1993).

Many aspects of the localization (or delocalization) of electron spin and charge in these radical cation salts are still unexplained. Thus, the single crystals of hexaperylene hexafluorophosphate $[(PE)_6PF_6]$, containing perylene dimers with strong intradimer but only weak interdimer interaction due to approximately parallel or orthogonal arrangement of the molecular planes, were of special interest. Crystal growth, crystal structure determination and relevant macroscopic physical properties of $(PE)_6PF_6$ are described below.

2. Experimental procedures and results

2.1. *Electrochemical crystal growth*

Electrocrystallization of $(PE)_6PF_6$ was achieved by anodic oxidation in a three-compartment electrochemical cell at 288 K using a saturated solution of perylene in tetrahydrofuran (THF), platinum-foil electrodes and constant voltage during 3 days [350 mg of perylene (zone-refined) and 1 g of Bu_4NPF_6 were dissolved in 100 ml THF]. Whereas a large voltage (*e.g.* 3.0 V) favours the growth of 2:1 needle-like 'metallic' crystals under these conditions, as was reported by Endres, Keller, Müller & Schweitzer (1985) before, for small voltages (2.0–2.1 V) and correspondingly small currents (7–14 μA) a preponderant portion of 6:1 squared-block-like 'semiconducting' crystals is obtained (total weight up to 20 mg). These crystals had glossy-black natural surfaces and did not show any sign of decomposition after 2 weeks in air at room temperature (m.p. *ca* 563–568 K, but decomposition starts at 513–528 K).

Table 1. *Crystal data and structure refinement*

Identification code	$(PE)_6PF_6$
Empirical formula	$C_{60}H_{36}F_3P_{0.50}$
Formula weight	829.37
Temperature (K)	213 (2)
Wavelength (Å)	0.71069
Crystal system	Triclinic
Space group	$P\bar{1}$
Unit-cell dimensions	
a (Å)	12.412 (4)
b (Å)	13.766 (5)
c (Å)	13.855 (5)
α (°)	110.63 (3)
β (°)	106.86 (3)
γ (°)	106.94 (3)
Volume (Å^3)	1904.6 (12)
Z	2
D_{calc} (Mg m^{-3})	1.446
Absorption coefficient (mm^{-1})	0.113
$F(000)$	861
Crystal size (mm)	0.45 × 0.38 × 0.30
θ range for data collection (°)	2.61–25.00
Index ranges	$-14 \le h \le 3$, $-16 \le k \le 16$, $-16 \le l \le 16$
Reflections collected	8536
Independent reflections	6637 ($R_{int} = 0.0217$)
Refinement method	Full-matrix least squares on F^2
Data/restraints/parameters	6637/0/719
Goodness-of-fit on F^2	1.058
Final R indices [$I > 2\sigma(I)$]	$R_1 = 0.0586$, $wR_2 = 0.1460$
R indices (all data)	$R_1 = 0.0930$, $wR_2 = 0.1617$
Extinction coefficient	0.0103 (13)
Largest diff. peak and hole (e Å^{-3})	0.801 and −0.350

2.2. *Crystal structure analysis*

A black-reddish as-grown crystal with well-developed crystal faces was mounted on a glass capillary and transferred to a Syntex P3 diffractometer with a PID-controlled nitrogen-gas stream cryostat set to 213 K (PID: proportional integral differential regulation). Further details of the data collection are given in Table 1. No absorption correction; refinements based on F^2, $w = 1/\sigma(F^2)$ in full-matrix least squares using the *SHELX*92 programs (Sheldrick, 1995); scattering factors taken from *International Tables for X-ray Crystallography* (1974), anomalous dispersion included. The structure was solved by direct methods. H-atom positions were freely refined with individual isotropic B values. The C and PF_6 positions were freely refined with individual anisotropic displacement parameters. Smooth convergence was achieved in a few least-squares cycles (max. shift/error < 0.01). The final agreement factors and the goodness-of-fit are given in Table 1. The final atomic positions are listed in Table 2.*

The structure consists of three almost orthogonal perylene molecules with a pseudo-threefold axis running parallel to the a-axis. The perylene molecules are quite planar with r.m.s. deviations of 0.015, 0.025

* Lists of structure factors, anisotropic displacement parameters, H-atom coordinates and complete geometry have been deposited with the IUCr (Reference: SH0048). Copies may be obtained through The Managing Editor, International Union of Crystallography, 5 Abbey Square, Chester CH1 2HU, England.

Table 2. *Atomic coordinates* ($\times 10^4$) *and equivalent isotropic displacement parameters* ($Å^2 \times 10^3$)

$U_{eq} = (1/3)\sum_i \sum_j U_{ij} a_i^* a_j^* \mathbf{a}_i . \mathbf{a}_j$.

	x	y	z	U_{eq}
P	0	0	0	35 (1)
F(1)	1322 (3)	977 (4)	737 (3)	173 (2)
F(2)	207 (4)	−340 (3)	−1090 (3)	144 (1)
F(3)	446 (5)	−827 (3)	297 (3)	163 (2)
C(1)	8281 (3)	8716 (3)	2328 (3)	42 (1)
C(2)	8610 (3)	8301 (3)	3066 (3)	43 (1)
C(3)	7724 (3)	7335 (3)	2978 (3)	37 (1)
C(4)	6491 (3)	6768 (2)	2155 (2)	30 (1)
C(5)	6127 (3)	7213 (2)	1385 (2)	30 (1)
C(6)	7040 (3)	8192 (2)	1477 (3)	34 (1)
C(7)	6688 (3)	8627 (3)	715 (3)	43 (1)
C(8)	5480 (4)	8116 (3)	−89 (3)	47 (1)
C(9)	4570 (3)	7150 (3)	−191 (3)	39 (1)
C(10)	4868 (3)	6679 (2)	521 (2)	30 (1)
C(11)	5561 (3)	5740 (2)	2041 (2)	30 (1)
C(12)	5856 (3)	5254 (3)	2741 (3)	36 (1)
C(13)	4961 (3)	4293 (3)	2647 (3)	42 (1)
C(14)	3761 (3)	3790 (3)	1844 (3)	39 (1)
C(15)	3402 (3)	4222 (2)	1083 (2)	31 (1)
C(16)	4299 (3)	5210 (2)	1179 (2)	28 (1)
C(17)	3933 (3)	5645 (2)	409 (2)	29 (1)
C(18)	2706 (3)	5084 (3)	−415 (3)	35 (1)
C(19)	1822 (3)	4098 (3)	−519 (3)	39 (1)
C(20)	2154 (3)	3675 (3)	216 (3)	38 (1)
C(21)	1989 (3)	7939 (3)	8609 (3)	45 (1)
C(22)	2715 (3)	8222 (3)	8099 (3)	47 (1)
C(23)	2669 (3)	7366 (3)	7147 (3)	41 (1)
C(24)	1890 (3)	6209 (2)	6693 (2)	31 (1)
C(25)	1133 (3)	5888 (2)	7230 (2)	31 (1)
C(26)	1191 (3)	6772 (3)	8201 (2)	35 (1)
C(27)	430 (3)	6457 (3)	8726 (3)	42 (1)
C(28)	−317 (3)	5328 (3)	8343 (3)	45 (1)
C(29)	−369 (3)	4461 (3)	7400 (3)	38 (1)
C(30)	323 (3)	4710 (2)	6827 (2)	31 (1)
C(31)	1797 (3)	5298 (2)	5657 (2)	29 (1)
C(32)	2472 (3)	5548 (3)	5076 (3)	38 (1)
C(33)	2373 (3)	4679 (3)	4095 (3)	41 (1)
C(34)	1607 (3)	3560 (3)	3696 (3)	37 (1)
C(35)	889 (3)	3245 (2)	4252 (2)	32 (1)
C(36)	978 (3)	4125 (2)	5248 (2)	29 (1)
C(37)	238 (3)	3802 (2)	5801 (2)	30 (1)
C(38)	−545 (3)	2647 (3)	5348 (3)	39 (1)
C(39)	−622 (3)	1790 (3)	4377 (3)	43 (1)
C(40)	83 (3)	2081 (3)	3845 (3)	39 (1)
C(41)	1851 (3)	8120 (3)	1954 (3)	41 (1)
C(42)	2303 (3)	7320 (3)	1682 (3)	41 (1)
C(43)	3145 (3)	7256 (3)	2548 (3)	37 (1)
C(44)	3536 (3)	7986 (2)	3705 (2)	30 (1)
C(45)	3074 (2)	8829 (2)	3998 (2)	28 (1)
C(46)	2218 (3)	8890 (2)	3101 (2)	33 (1)
C(47)	1772 (3)	9729 (3)	3386 (3)	37 (1)
C(48)	2143 (3)	10481 (3)	4510 (3)	38 (1)
C(49)	2975 (3)	10421 (3)	5386 (3)	34 (1)
C(50)	3450 (3)	9613 (2)	5163 (2)	28 (1)
C(51)	4408 (3)	7924 (2)	4617 (2)	29 (1)
C(52)	4896 (3)	7122 (3)	4390 (3)	35 (1)
C(53)	5741 (3)	7075 (3)	5267 (3)	41 (1)
C(54)	6123 (3)	7831 (3)	6388 (3)	42 (1)
C(55)	5650 (3)	8649 (3)	6676 (2)	34 (1)
C(56)	4781 (3)	8704 (2)	5784 (2)	30 (1)
C(57)	4312 (3)	9540 (2)	6079 (2)	29 (1)
C(58)	4705 (3)	10266 (3)	7230 (3)	37 (1)
C(59)	5553 (3)	10211 (3)	8101 (3)	44 (1)
C(60)	6028 (3)	9425 (3)	7835 (3)	41 (1)

and 0.014 Å for perylene I [C(1)–C(20)], II [C(21)–C(40)] and III [C(41)–C(60)], respectively (Fig. 1). Dimer formation, which is important in the 3:1 and 2:1 salt (Endres, Keller, Müller & Schweitzer, 1985), is also observed in the 6:1 salt. In the unit cell shown in Fig. 1, the pairs of parallel molecules belong to different dimers and are quite a long way shifted apart in a lateral direction. Therefore, Fig. 2 demonstrates the dimer formation more clearly. Intradimer separation of the PE molecules is much smaller than the separation from one to the next PE dimer [d(I–I′) = 3.23/4.36, d(II–II′) = 3.36/4.64 and d(III–III′) = 3.33/3.85 Å]. The atomic arrangement of $(PE)_6PF_6$ is very similar to that in hexaperylene perchlorate (Endres, Keller, Müller & Schweitzer, 1985). The typical positional differences between the two structures are a few hundredths of an Å; note that the origin in Endres *et al.* is shifted by $0,0,\frac{1}{2}$. The smearing of the F atoms is quite pronounced and indicates strong librations and/or positional disorder. The mean P—F distance (1.529 Å), however, is still fairly close to the expected value of 1.579 Å (*International Tables for Crystallography*, 1992) and indicates that the PF_6 group is not freely rotating;

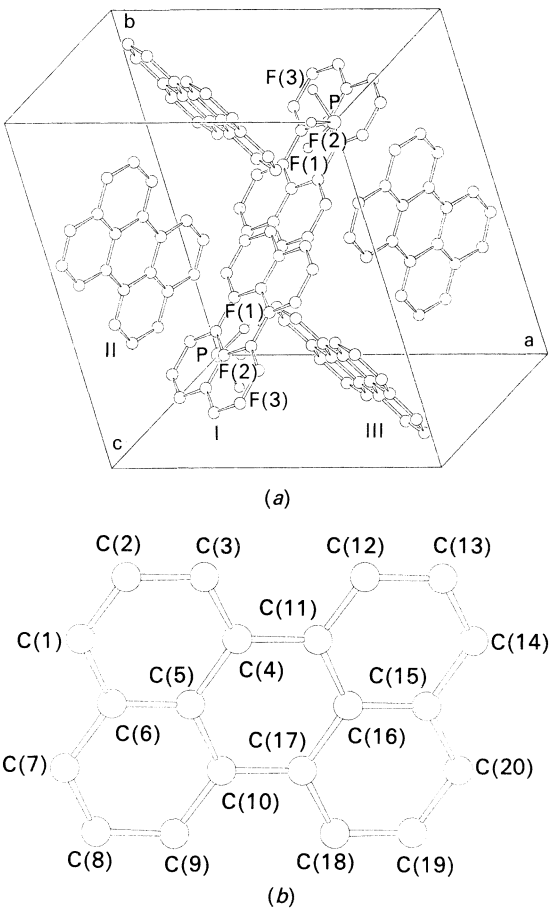

Fig. 1. Crystal structure of $(PE)_6PF_6$. (*a*) Mutually perpendicular arrangement of the six perylene molecules (I, II, III) in the unit cell. (*b*) Numbering scheme of perylene I; the numbering of the atoms in the perylene II and III molecules corresponds to this scheme [*i.e.* C(21), C(22) *etc.* and C(41), C(42) *etc.* analogous to C(1), C(2) *etc.*].

the librational r.m.s. amplitudes are, however, quite large – of the order 10–15°. The anisotropic displacement parameters of the C atoms are quite normal and consistent with a fully ordered structure.

2.3. *Magnetic susceptibility*

The static (total) magnetic susceptibility of $(PE)_6PF_6$ was determined with a SQUID magnetometer (Quantum Design MPMS) for a magnetic field strength of 20 kOe in the temperature range 1.8–200 K. During the measurements, the sample consisting of many single crystals at arbitrary orientation and weighing *ca* 21.1 mg was surrounded by a low-pressure helium atmosphere. The temperature dependence of the molar susceptibility χ_m and of $\chi_m T$ is shown in Fig. 3. Except for temperatures below 15 K, where magnetic saturation is responsible for deviation from the Curie–Weiss law and for a small anomaly at *ca* 40 K, χ_m can be accurately decomposed into paramagnetic and diamagnetic contributions

$$\chi_m = C/(T-\Theta) + \chi_m^{\text{dia}} = xN_A g^2 \mu_B^2 S(S+1)\{3k_B(T-\Theta)\}^{-1} + \chi_m^{\text{dia}}, \quad (1)$$

with Curie constant C, asymptotic Curie temperature Θ, x the portion of 'active' radical spins, Avogadro's number N_A, $g = 2$, $S = \frac{1}{2}$, Bohr magneton μ_B and Boltzmann constant k_B.

The diamagnetism $\chi_m^{\text{dia}} = -(937 \pm 21) \times 10^{-6}$ e.m.u. mol^{-1} determined from the fit in Fig. 3 is 12% weaker than according to an estimate from tabulated data for the orientational average, *i.e.* $-(1066 \pm 36) \times 10^{-6}$ e.m.u. mol^{-1} (Gupta, 1986).

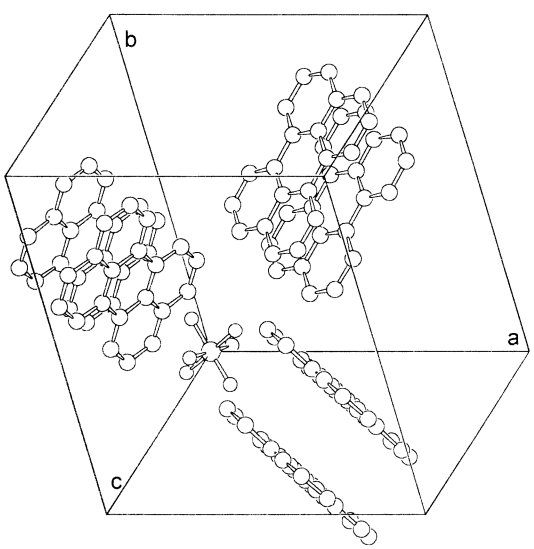

Fig. 2. Six perylene molecules of $(PE)_6PF_6$ selected to show the arrangement of the PE dimers in the cell orientation of Fig. 1(*a*).

The fit value $\Theta = -(0.18 \pm 0.01)$ K, residing at the error limit of the analysis indicates very weak antiferromagnetic interactions. Such interactions are also revealed by the deviation of the experimental data from the straight line fit to $\chi_m T$ in Fig. 3, visible for temperatures between 10 and 40 K. Relating the fit value $C = (0.367 \pm 0.002)$ e.m.u. K mol^{-1} with the calculated value $C = x0.375$ e.m.u. K mol^{-1} indicates that (98 ± 1)% of the free spins predicted for the 6:1 stoichiometry of this radical cation salt are actually observed.

2.4. *Electrical conductivity*

The electrical conductivity of $(PE)_6PF_6$ is small and therefore has been derived by the two-probe method. The experimental data of two different crystals are presented in Fig. 4 as a function of temperature and of inverse temperature, and in Fig. 5 on a doubly logarithmic scale. The small steps in the experimental curves result from switching of the constant measuring voltage and reveal weak nonlinearities. It is surprising that the electrical conductivity obeys a powder law $\sigma = AT^B$, with $B \approx 14$

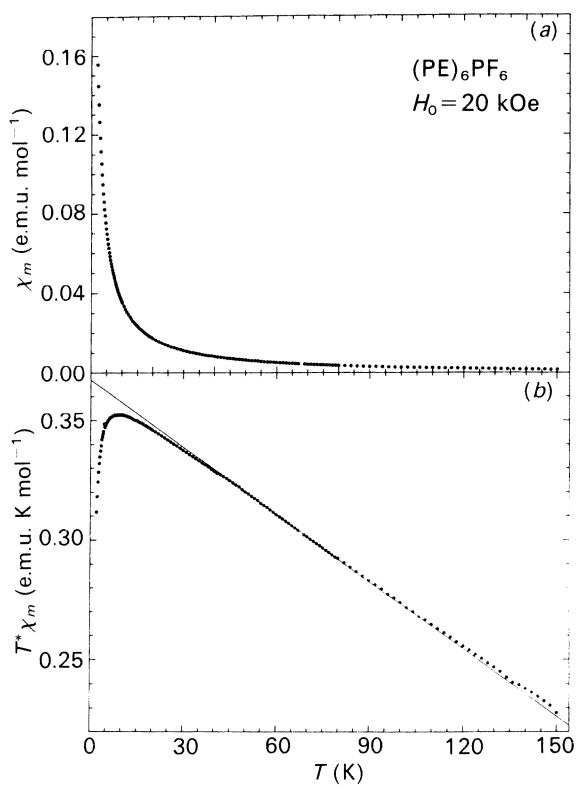

Fig. 3. Magnetic susceptibility of $(PE)_6PF_6$ as a function of temperature. (*a*) The total magnetic susceptibility χ_m was measured at 20 kOe field strength (same temperature scale as below). (*b*) The deviation of the product $\chi_m T$ from the straight line reveals weak antiferromagnetic interactions and magnetic saturation at low temperatures.

over 10 decades of the conductivity. In the discussion of electrical transport in polyacetylene, comparably large exponents were discussed in conjunction with the phonon-assisted hopping of electrons between soliton sites (for random distribution of impurities and thus essentially three-dimensional conduction pathways; Kivelson, 1982; Epstein, Rommelmann, Abkowitz & Gibson, 1981).

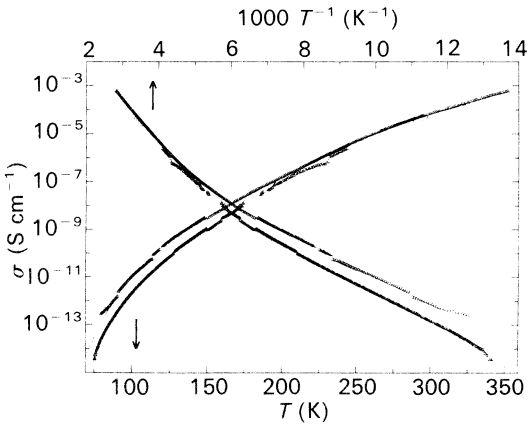

Fig. 4. Electrical conductivity of two different single crystals of $(PE)_6PF_6$ (arbitrary direction) as a function of the temperature (lower scale) or the reciprocal temperature (upper scale). The solid line fit is explained in the text.

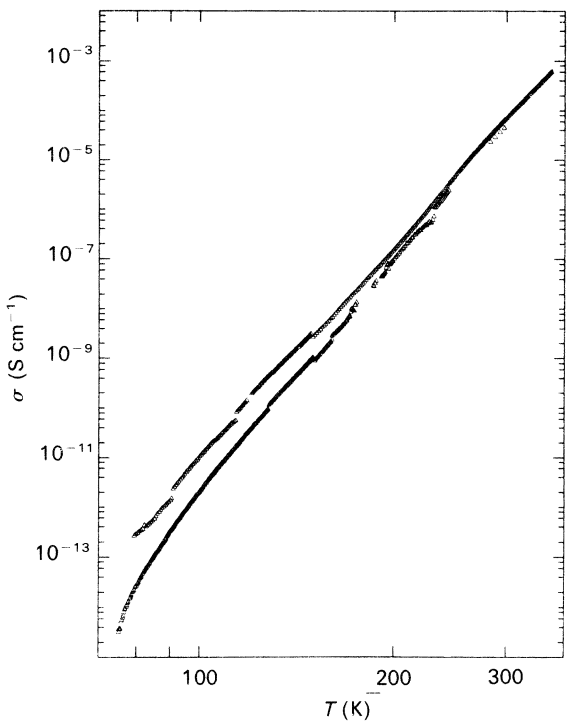

Fig. 5. Conductivity data of $(PE)_6PF_6$ single crystals (Fig. 4) on a doubly logarithmic scale.

The solid line fits in Fig. 4 show that the data can also be reasonably described by the superposition of two thermally activated conductivity processes

$$\sigma(T) = \sigma_L \exp(-\Delta_L/k_BT) + \sigma_H \exp(-\Delta_H/k_BT). \quad (2)$$

The parameters $\sigma_L = (2.0 \pm 1.2) \times 10^{-4}$ S cm^{-1}, $\sigma_H = 26$ S cm^{-1}, $\Delta_L/k_B = (1734 \pm 6)$ K ($\Delta_L =$ 149 me V) and $\Delta_H/k_B = 3875$ K ($\Delta_H = 334$ me V) were derived. The order of magnitude of these activation energies is typical for semiconducting radical cation salts of arenes (Raible *et al.*, 1993). Since deviations from ideal stoichiometry may amount to $(2 \pm 1)\%$, according to the magnetic characterization, it is obvious to assume that defect and intrinsic conductivity processes are reflected by the two contributions in (2).

3. Concluding remarks

The three-dimensional crystal structure of the radical cation salt $(PE)_6PF_6$ contains PE dimers with a very small intradimer separation, as is also typical for the 'metallic' PE salts, but a large separation from one to the next parallel PE dimer (see Fig. 2 for the intradimer and Fig. 1 for the interdimer separation). Three independent dimers are accommodated in the unit cell with an almost orthogonal orientation of their molecular planes. This results in only weak interdimer interaction. The static magnetic susceptibility supports the description of $(PE)_6^{\cdot+}PF_6^-$ as a magnetic semiconductor with one 'localized' Curie-like radical spin $S = \frac{1}{2}$ per formula unit, indicative of the importance of Coulomb correlations in this salt. The asymptotic Curie temperature or, in other words, the resultant exchange coupling of one spin with all the neighbouring spins is weak. Nevertheless, the small ESR linewidth of only *ca* 1 Oe reveals the action of a narrowing mechanism for the electron-spin dipole–dipole and hyperfine contributions to the linewidth in $(PE)_6PF_6$. The electrical conductivity characterizes $(PE)_6PF_6$ as an organic semiconductor with comparatively large activation energy and presumably a non-neglegible influence of defects.

We thank D. Schweitzer and J. Gmeiner for a thorough introduction into electrochemical crystal growth and also J. Gmeiner for the preparation of the zone-refined perylene. This work was supported by the Deutsche Forschungsgemeinschaft within the Sonderforschungsbereich 195 (Universität Karlsruhe).

References

ENDRES, H., KELLER, H. J., MÜLLER, B. & SCHWEITZER, D. (1985). *Acta Cryst.* C**41**, 607–613.

ENKELMANN, V. & GÖCKELMANN, K. (1987). *Ber. Bunsenges. Phys. Chem.* **91**, 950–957.

EPSTEIN, A. J., ROMMELMANN, H., ABKOWITZ, M. & GIBSON, H. W. (1981). *Mol. Cryst. Liq. Cryst.* **77**, 81–96.
GUPTA, R. R. (1986). Landolt-Börnstein, *New Series II*/16, edited by K.-H. HELLWEGE & A. M. HELLWEGE, pp. 176–177, 436–437. Berlin: Springer.
KELLER, H. J., NÖTHE, D., PRITZKOW, H., WEHE, D., WERNER, M., KOCH, P. & SCHWEITZER, D. (1980). *Mol. Cryst. Liq. Cryst.* **62**, 181–200.
KIVELSON, S. (1982). *Phys. Rev. B*, **25**, 3798–3821.
RAIBLE, CH., GMEINER, J., WINTER, H., DORMANN, E., STENGER-SMITH, J. D. & ENKELMANN, V. (1993). *Synth. Met.* **59**, 71–80.
RIESS, W., BRÜTTING, W. & SCHWOERER, M. (1993). *Synth. Met.* **55–57**, 2664–2669.
SHELDRICK, G. M. (1995). *SHELX*92. *An Integrated System for Solving, Refining and Displaying Crystal Structures from Diffraction Data. J. Appl. Cryst.* In preparation.

Acta Cryst. (1994). B**50**, 746–762

The Influence of the Nitro Group on the Solid-State Structure of 4-Nitropyrazoles: the Cases of Pyrazole, 3,5-Dimethylpyrazole, 3,5-Di-*tert*-butylpyrazole and 3,5-Diphenylpyrazole. I. Static Aspects (Crystallography and Thermodynamics)

BY ANTONIO L. LLAMAS-SAIZ, CONCEPCIÓN FOCES-FOCES AND FÉLIX H. CANO

Departamento de Cristalografía, Instituto de Química-Física 'Rocasolano', CSIC, Serrano 119, *E*-28006 *Madrid, Spain*

PILAR JIMÉMEZ AND JOSÉ LAYNEZ

Instituto de Química-Física 'Rocasolano', CSIC, Serrano 199, *E*-28006 *Madrid, Spain*

WIM MEUTERMANS AND JOSÉ ELGUERO

Instituto de Química Médica, CSIC, Juan de la Cierva 3, *E*-28006 *Madrid, Spain*

AND HANS-HEINRICH LIMBACH AND FRANCISCO AGUILAR-PARRILLA

Institut für Organische Chemie, Fachbereich Chemie, Freie Universität Berlin, Takustrasse 3, *D*-14195 *Berlin, Germany*

(*Received* 31 *January* 1994; *accepted* 19 *April* 1994)

Abstract

We have determined the enthalpies of sublimation of 3,5-di-*tert*-butylpyrazole (3), 3,5-diphenylpyrazole (4), 4-nitropyrazole (5), 3,5-dimethyl-4-nitropyrazole (6), 3,5-di-*tert*-butyl-4-nitropyrazole (7) and 3,5-diphenyl-4-nitropyrazole (8); those of pyrazole (1) and 3,5-dimethylpyrazole (2) were already known. The effect of the C-substituents (Me, Bu^t, Ph and NO_2) on the enthalpies of sublimation of pyrazoles and benzenes are additive and linearly related. Moreover, we report the structure of three of these 4-nitropyrazole derivatives, (5), (7) and (8), which have been solved by X-ray crystallography; those of the remaining five compounds were already known. Except for (8), there appears to be an opening of the intramolecular angle at C(4) due to the presence of the nitro group, that, on the other hand, seems to have no correlation with the presence of the hydrogen H(1)/H(2) disorder. Crystal structure diagrams and intermolecular contacts were analysed for either pyrazole derivatives with and without nitro substituents. There appear to be two general modes of packing: the first is based upon a secondary structure of trimers in sheets, which distorts into helices; the second is made of dimers, which then pack into sheets. The nitro group seems to have no influence in the packing, which is more controlled by the substituents at C(3) and C(5). Although only partly successful, we have established some relationships between crystallographic results and thermodynamic properties. First, between the planarity or not of the 4-nitro group and the acid and basic pK_a's, and second, between some packing descriptors and the sublimation enthalpies.

Introduction

We are in the process of carrying out a systematic study of the properties of NH-pyrazoles in the solid state by X-ray crystallography (Llamas-Saiz, Foces-